

Preparation and comparison of electrospun PEO/PTFE and PVA/PTFE nanofiber membranes for syringe filters

Cigdem Akduman 

Pamukkale University, Denizli Vocational School of Technical Sciences, Department of Textile Technology, Denizli, Turkey

Correspondence

Cigdem Akduman, Pamukkale University, Denizli Vocational School of Technical Sciences, Department of Textile Technology, 20160, Denizli, Turkey.
Email: cakduman@pau.edu.tr

Abstract

The fabrication of a high-performance PTFE membrane remains challenging and still under interest. Electrospinning is one of the possible fabrication methods for PTFE membranes. But, due to the high solvent resistance and the high melt viscosity, PTFE emulsion should be blended with a carrier polymer solution and then it can be electrospun. In this study, PTFE membranes were produced with four different ratios of PVA and PEO polymers as carrier and then sintered at 380°C, to left only PTFE nanofibers behind. Produced hydrophobic PTFE membranes' WCA values were between 120-132° for PEO/PTFE nanofibers and 112-124° for PVA/PTFE nanofibers. SEM images revealed that PEO/PTFE membranes preserved their fibrous structure better. After sintering, diameter of 7PEO/PTFE, 8PEO/PTFE, 9PEO/PTFE, and 10PEO/PTFE nanofibers were 612, 818, 822, and 923 nm, respectively. Only 30PVA/PTFE nanofibers showed some fiber structure after sintering with evenly distributed pores. PEO/PTFE membranes were thicker than commercial syringe filter membranes and PVA/PTFE membranes and was about 0.24 μm. Although mean pore size measurements of both PEO/PTFE and PVA/PTFE membranes were 0.90 and 1.07 μm, respectively and higher than commercial membranes, bacterial removal tests of PEO/PTFE membrane were promising and close to commercial syringe filter results with 1.3 3log CFU/mL.

KEYWORDS

bacterial removal, electrospinning, nanofibers, polytetrafluoroethylene, syringe filters

1 | INTRODUCTION

Syringe filters are single-use filters that are attached to the end of a syringe and are generally used for effective and fast filtering, sterilization, and material purification, the removal of particulate impurities or contamination from liquid and gas samples before analysis in many laboratories.^{1,2} Porous membranes are the key component of these syringe filters. Ultra-fine

or nanoscale fibrous, porous polymeric membranes have a thin layer of semi-permeable materials.^{3,4} They are matched by composition, pore size, filter diameter and the selection of these filters are made according to the application.²

Polytetrafluoroethylene (PTFE) is one of the widely used membrane in syringe filters due to its excellent hydrophobicity, chemical stability, high heat resistance, low protein binding, and high fracture toughness⁵⁻⁷ and

This is an open access article under the terms of the [Creative Commons Attribution](https://creativecommons.org/licenses/by/4.0/) License, which permits use, distribution and reproduction in any medium, provided the original work is properly cited.

© 2023 The Author. *Journal of Applied Polymer Science* published by Wiley Periodicals LLC.

can be used for various liquid and gas separation application.^{3,7–10} Its distinctive molecular structure gives desired chemical, physical, electric, antifriction, and other properties^{11,12} that are unique for PTFE material.

However, porous PTFE membranes are challenging to fabricate by common phase inversion or melt spinning methods¹⁰ because PTFE has high melt viscosity, negligible solubility which makes it difficult to process using conventional processing techniques.^{3,6,13} Due to its specific processing needs, stretching, sintering, wrapping, electrospinning, and near field electrospinning methods can be employed in the fabrication of PTFE membranes.¹⁴ But PTFE expansion and sintering processes remain the main commercial techniques for the manufacture of porous PTFE membranes.^{15–17} The final properties are affected from sintering cycle profiles of time and temperature.¹⁸ Expansion process involves extrusion, followed by stretching to form microporous films. These expanded PTFE membranes are called e-PTFE membranes are usually prepared by uniaxial or biaxial stretching^{13,14,19} to achieve a higher specific surface area, which provides high gas permeability and more contact area between the particles and fibers, while providing sufficient particle retention.⁵ However, the stretching technologies generally suffered from wide pore size distribution, low porosity at small thickness of membranes.²⁰ Moreover, PTFE biaxial stretching porous membrane generally needs a supporting layer such as a nonwoven layer because of its strength and weaknesses.¹⁴

Therefore, the fabrication of a high-performance PTFE membrane continues to be difficult and still under interest. With the increasing utilization of electrospinning and nanofibers, development of PTFE nanofibers by electrospinning draws more attention and can be alternative production method for porous PTFE membranes. Electrospinning is still novel method to produce various porous membranes from polymer solutions, melts, and emulsions. However, because of high solvent resistance and the high melt viscosity, PTFE emulsion is blended with a carrier polymer solution such as poly(vinyl alcohol) (PVA)^{3,6,12,21–23} and polyethylene oxide (PEO) for electrospinning.^{24–28} Subsequently, a sintering step is performed to fuse the PTFE particles into continuous PTFE fibers by eliminating the carrier polymer.¹⁴

Xiong et al. blended PVA and PTFE emulsion with different mass concentrations and electrospun into composite nanofibers and then sintered at 390°C. They investigated the influence of the blend ratio of PVA to PTFE and electrospinning parameters on the morphology and diameter of the PTFE nanofibers and evaluated their tensile strength. When the mass ratio of PVA to PTFE was 30:70, smooth fibers were obtained. After sintering, DSC analysis and ATR-FTIR spectra confirmed

the complete decomposition of PVA.⁶ Zhou et al. investigated the effects of sintering temperature and time on the morphology and properties of the PTFE/PVA membranes. They achieved moniliform fiber network with a water contact angle above 150°, porosity about 80% and applicable strength. Produced membranes displayed a stable salt rejection above 98.5% for 10 h operation when the feed NaCl concentration was 3.5%.²¹

Kang et al. and Xu et al. prepared a mixture of PTFE, PVA, boric acid (BA) for electrospinning.^{13,23} Kang et al. dried the PTFE/PVA/BA composite fiber membrane for 5–6 h at 70°C and then sintered at several temperatures (320–420°C) for 20 min at a heating rate of 10°C/min in air atmosphere to obtain the pure PTFE nanofiber membrane, Xu et al. used nitrogen atmosphere. Kang et al. obtained PTFE nanofibers with diameters of 200 nm to 1000 nm after calcinating. They showed by using the gel-spinning solution of PTFE/PVA/BA, PTFE nanofiber membranes could be electrospun.¹³ Xu et al. evaluated these composite membranes in air filtration and obtained 98% filtration efficiency and 90 Pa of low pressure drop and self-cleaning properties.²³ Huang et al. used electrospun poly(acrylonitrile) (PAN) nanofibers to reinforce the PTFE/PVA composite membranes to prevent the shrinkage which occurs after sintering.³

Son et al. prepared PTFE–PEO electrospinning solutions to determine the optimized condition. As the ratio of the PEO increases, the fiber structure improves. For oil/water separation, produced membrane had 143.6° of water contact angle and 0° of oil contact angle.²⁸ Huang et al. also produced PTFE/multiwalled carbon nanotubes (CNT) nanofiber membranes using PEO as carrier polymer. Produced PTFE/CNT (5 wt%) membranes showed the increased conductivity of 1.5 S/m.²⁷ Lin et al. applied thermal treatment at 350°C to remove the PEO component from the electrospun PTFE-PEO nanofibers. Produced PTFE membranes showed good electret properties, effective ability of converting mechanical energy into electricity with a peak power of 56.25 μW and long-term cycling stability, as a sensitive self-powered wearable.²⁶ Su et al. prepared PTFE hollow fiber from PTFE/PEO emulsion electrospinning and calculated the permeate flux of the membranes as 4.6–8.8 times higher than the commercial PTFE stretching membranes.²⁵

Another approach for production of PTFE membrane is adding PTFE micro-powders to the spinning solution. In order to improve the surface hydrophobicity of the nanofiber membrane, Dong et al. added PTFE micro-powders to the PVDF solutions. PTFE micro-powder ratios of 0, 3, 6 and 12 wt.% were used. The addition of PTFE reduced the surface energy of the membranes and improved the surface roughness along with the surface hydrophobicity.²⁹

Although several researchers have studied the electrospun PTFE membranes, comparison of the carrier polymer and the evaluation of these membranes in syringe filters for bacterial removal have not been studied as per author knowledge. PTFE syringes consist of a housing with a membrane which serves as a filter. Pressure is applied across the membrane for this purpose. They are useful in the removal of specific impurities, including bacterial contamination from the fluid samples. In products that are denatured when temperature is applied, syringe filters are preferred to remove bacterial contamination. In this way, proteins and other substances are not denatured. This application is used in the preparation of serum, apheresis, or a valuable antibiotic. In this study PTFE membranes were produced using both PVA and PEO as carrier polymer and then sintered. Prepared PTFE membranes were characterized with scanning electron microscope (SEM), thermogravimetric analysis (TGA) and Fourier transform infrared (FTIR) analysis. For determination of hydrophobicity of the PTFE nanofiber membranes, the water contact angles (WCA) of each membrane were measured. Then selected PEO/PTFE and PVA/PTFE concentrations were electrospun to produce thicker PTFE nanofiber membranes and were compared with commercial 0.2 and 0.45 μm syringe filters in means of pore size and bacteria removal efficiency. For bacterial removal efficiency, these PTFE membranes were placed in a 3D printed syringe filter housing and evaluated for the first time.

2 | EXPERIMENTAL

2.1 | Materials

PEO, Polyox WSR N750 is pharmaceutical grade, and a trademark of Dow Chemical Company, with approximate molecular weight of 300,000. It was provided Hifyber as a gift. PVA, average molecular weight of $\sim 125,000$ g/mol (CAS Number: 9002-89-5), 1,2,3,4-butanetetracarboxylic acid (BTCA, CAS Number: 1703-58-8) and sodium hypophosphite monohydrate ($\text{NaPO}_2\text{H}_2\cdot\text{H}_2\text{O}$, CAS Number: 10039-56-2) were purchased from Sigma Aldrich Chemical Company. PTFE dispersion used in this study is Teflon™ PTFE DISP 33. It is a milky white aqueous PTFE dispersion

stabilized with a non-ionic surfactant. Solids Content (% PTFE by weight) is 61%. Melting point of the resin particles is approximately at 337°C.³⁰ Commercial 0.2 and 0.45 μm syringe PTFE filters were purchased from Millex (Milipore) and Isolab and coded with SF0.2 and SF0.45, respectively.

2.2 | Preparation of electrospinning solutions

A 10% PEO stock solution was prepared by dissolving PEO powder by vigorous stirring, PEO powder was sprinkled over the water and stirred about 600 rpm for 1 min, then rpm was decreased to about 60. Stirring was continued for 30 min to 1 h until the solution appears homogeneous.³¹ For 10% PVA solution, PVA powder stirred for at least 2 h at 80°C in distilled water at room temperature. BTCA was directly added into the spinning solution with sodium hypophosphite monohydrate as a catalyst in ratio of 2:1 (w/w) and stirred further 15 min. BTCA is generally used for crosslinking purposes via esterification^{32,33} at about 150–180°C. It also enhances the conductivity of the PVA solution, thus improves the spinnability of the polymer solution. Since in this study all nanofibers are sintered, it is added just for enhancing the spinnability. Total polymer ratios, the amount of PVA, PEO and PTFE dispersion were given in Tables 1 and 2. Distilled water was also added to achieve the 7/93, 8/92 and 9/91 PEO/PTFE solution concentration. Conductivity measurement of the spinning solutions were carried out using J.P. Selecta Conductivity meter, CD-2004.

2.3 | Electrospinning

Electrospinning of the polymer solutions was carried out by a set-up consisting of a flat tip stainless steel needle mounted on a syringe pump (Inovenso), grounded rotating metal drum collector and a high voltage supply (Pulse Techtronic). PEO/PTFE and PVA/PTFE solutions were electrospun at voltage of 13 and 15 kV, respectively. Tip-to-collector distance of 15 cm, feeding rate of 0.6 mL/h were used for all solutions. 40 mesh chromium sieve wire was used as a deposition material because of

TABLE 1 Preparation of PEO/PTFE solutions.

Sample coding	Total polymer ratio	PEO/PEO solution (g/g)	PTFE/PTFE solution(g/g)	Distilled water (g)	Total solution(g)
7PEO/PTFE	7/93 PEO/PTFE	0.7/7	9.3/15.5	2.5	25
8PEO/PTFE	8/92 PEO/PTFE	0.8/8	9.2/15.33	1.67	25
9/PEO/PTFE	9/91 PEO/PTFE	0.9/9	9.1/15.17	0.83	25
10PEO/PTFE	10/90 PEO/PTFE	1/10	9/15	—	25

TABLE 2 Preparation of PVA/PTFE solutions.

Sample coding	Total polymer ratio	PVA/PVA solution (g/g)	PTFE/PTFE solution (g/g)	Total solution (g)
10PVA/PTFE	10/90 PVA/PTFE	1.5/15	13.5/22.5	37.5
20PVA/PTFE	20/80 PVA/PTFE	1.5/15	6/10	25
25PVA/PTFE	25/75 PVA/PTFE	1.5/15	4.5/7.5	22.5
30PVA/PTFE	30/70 PVA/PTFE	1.5/15	3.5/5.83	20.83

the sintering process. For the sintering process, the deposition material must be resistant to high temperatures, so some researchers have used glass tubes, but it is not possible to set the glass as desired in the deposition area. For this reason, chromium sieve was preferred in this study. The chromium sieve can be wrapped around the drum collector and then maintain the given shape, it is also conductive and can be grounded. After electrospinning nanofibers can be directly sintered with chromium sieve.

All solutions were produced for 1 h, and selected PEO/PTFE and PVA/PTFE solutions (10PEO/PTFE and 30PVA/PTFE) were produced for 5 h for thicker membranes for bacterial removal evaluation.

2.4 | Sintering process

PTFE fiber membranes were dried for 6 h at 70°C to prevent the shrinkage and then were sintered at 380°C. The sintering process was carried out in a high-pure nitrogen atmosphere with a gas flow rate of 200 $\mu\text{L}/\text{min}$. The furnace was first heated to 380°C with a heating rate of 4°C/min and held for 10 min for sintering. During the sintering process, a N_2 atmosphere was maintained.

2.5 | Thermal properties

The thermal behavior of electrospun PEO, PVA, PEO/PTFE and PVA/PTFE nanofibers were investigated by TGA (PERKIN ELMER TGA-4000) by heating samples from 25 to 600°C at a rate of 10°C/min under a continuous nitrogen purge at a rate of 20 mL/min. Selected PEO/PTFE-5 h and PVA/PTFE-5 h nanofibers were also investigated after sintering process.

2.6 | The WCA measurements

For determination of hydrophilicity of the PTFE nanofiber membranes, the WCA were measured by using CAM 200 contact angle meter (KSV Instruments, Helsinki, Finland). The contact angles with distilled water were measured on the upper surface of the electrospun nanofiber membranes which were separated from the

chromium sieve before measurements. The measurements were conducted room temperature (25°C) and at a relative humidity of 40–50%. A droplet of water with a volume of 2 μL was deposited onto the membrane surface from 5 cm by vibrating the tip of a micro-syringe. A real-time camera captured the image of the droplet. The droplet was recorded on the membrane surface after 9 s.

2.7 | SEM analysis

The morphologies of the PEO, PVA, PEO/PTFE and PVA/PTFE nanofibers were characterized using SEM (FEI Quanta 250 FEG). Each sample was coated with a thin film of gold using an Emitech K550X ion sputtering device prior to SEM observation for 2 min. The mean diameter of the resultant fibers was calculated from measurements of SEM images by using the Image J program. Fiber diameters were measured by drawing straight lines perpendicular to the fiber axis. Approximately thirty measurements were carried out from different parts of each sample.

2.8 | FTIR measurements

Fourier transform infrared spectroscopy (FTIR) analysis is carried out by using a ThermoScientific FTIR spectrometer. After sintering of PEO/PTFE-5 h and PVA/PTFE-5 h membranes, the elimination of the PEO and PVA component from the nanofibers was analyzed. Scans were obtained in a spectral range from 650 to 4000 cm^{-1} .

2.9 | Thickness measurements

The thickness of the PEO/PTFE and PVA/PTFE nanofiber membranes were measured by Mitutoyo digital micrometer at 0.01 mm accuracy. Four measurements were carried out from the different parts of each sample.

2.10 | Pore size measurements

The pore size and pore size distribution of the CA nanofiber membranes were measured by capillary flow porometry

(Porolux 1000- Germany). All samples were wetted by Galpore 16 (a wetting liquid with a low surface tension of 16 dyne/cm) and then tested. The mean pore size was calculated from wet, dry and half dry conditions for commercial syringe filters SF0.2 and SF0.45, besides selected PEO/PTFE-5 h and PVA/PTFE-5 h nanofiber membranes for comparison. Mean flow pore size (MFP), first bubble point (FBP), were measured by wet-up/dry-up method and the analysis was done by using Automated Capillary Flow Porometer system software.

2.11 | 3D printing of syringe filter housing

Syringe filter housings were printed by 3D printer (Wanhao Duplicator i3 Mini), Figure 1a. PLA filaments were used, filling ratio was 100% and, wall thickness was 0.8 mm. The lower and upper housings (Figure 1b,c) were separately printed and bonded with heat after the membrane placement (Figure 1d). In fact, polypropylene or high-density polyethylene is used as a housing material in commercial syringe filters, but in our study only bacteria filtration was the case, and heavy acidic, basic conditions or high temperatures was not considered, PLA polymer was used which was easy to work with in 3D printers. Only 10PEO/PTFE and 30PVA/PTFE membranes were selected and produced for 5 h then were placed inside the printed syringe filter housing.

2.12 | The removal of bacteria by PTFE syringe filters

Escherichia coli American Type Culture Collection (ATCC) 25,922, was used for bacteria removal studies. It

was prepared 8log colony-forming units per milliliter (CFU/mL) and diluted to 4log CFU/mL. 10 mL, 4log CFU/mL *Escherichia coli* solutions were filtered with PEO/PTFE-5 h and PVA/PTFE-5 h syringe filters and 0.2 (SF0.2) and 0.45 (SF0.45) μm commercial syringe filters for comparison. Pressure was applied by hand. After filtration, microbiological cultivation is done in a nutrient agar culture medium at 30°C and then the bacterial CFU was counted and compared with the blind solution.

3 | RESULTS AND DISCUSSION

3.1 | Conductivity results of electrospinning solutions

The conductivity of the electrospinning solution is directly affecting the spinnability of the nanofibers. Although both PEO and PVA polymers are easy to electrospin, some researchers add salt to increase the conductivity. In this study pH of the PTFE dispersion was 10 and had conductivity. Thus, conductivity of the PEO/PTFE solutions increased with the increased PTFE content. On the other hand, a carboxylic acid, BTCA, was added to PVA solutions to achieve crosslinking and increase the spinnability which also affect the conductivity of the PVA/PTFE solutions. Therefore, with the increasing PVA content, conductivity of the PVA/PTFE solutions increased much more when compared to PEO/PTFE solutions (Table 3).

3.2 | Thermal properties of nanofibers

Sintering removes the carrier polymer by thermal degradation and high sintering temperature allows the PTFE

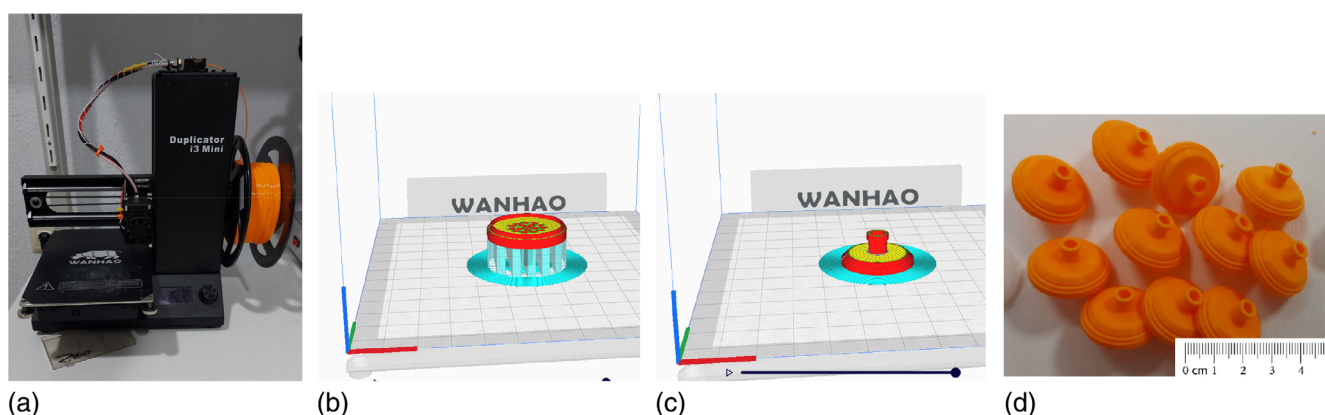


FIGURE 1 (a) 3D printer with PLA filament, (b) lower (c) upper housing part, (d) printed syringe filter with a membrane. [Color figure can be viewed at [wileyonlinelibrary.com](https://onlinelibrary.wiley.com)]

particles to melt and fused together and enables the formation of pure PTFE nanofibers. Figure 2a,b represent the TGA curves of pure PEO and PEO/PTFE nanofibers, PVA and PVA/PTFE nanofibers before sintering, respectively. Derivative TG (DTG) curves were given in supplementary file in Figure S1 and Figure S2. In Figure 2a, for neat PEO nanofibers, the TGA thermogram curve revealed that the single mass-loss step occurred in the range of 344–440°C, with a main weight loss, onset temperature of ~344°C, inflection point of 405°C (Figure S1) and a residual weight of less than 1% at 600°C. For the composite PEO/PTFE nanofibers, the thermograms showed an expected two-step mass loss, corresponding to the decomposition of PEO and PTFE phases. A weight loss occurred between 170–220°C due to residual of surfactants.^{12,13} In the composite membrane, the peak weight-loss temperature for the PEO component is

TABLE 3 Conductivity of PEO/PTFE and PVA/PTFE solutions.

PEO/PTFE and PVA/PTFE solutions	Conductivity ($\mu\text{S}/\text{cm}$)
7PEO/PTFE	1010
8PEO/PTFE	983
9/PEO/PTFE	940
10PEO/PTFE	896
10PVA/PTFE	2460
20PVA/PTFE	2720
25PVA/PTFE	2840
30PVA/PTFE	2960

slightly lower and about 380°C when compared to the pure PEO, which can arise due to the interfacial effects between the PTFE and PEO components. Corresponding to the decomposition of PTFE, the second mass loss started onset temperatures of about 510°C, which was also observed by Zhao et al.²⁴ Looking at the TGA results, the PEO part mainly decomposed about 380°C and the PTFE component of the membrane steady up to ~450°C. At temperatures higher than 510°C, thermal degradation of PTFE began and that represents the highest sintering temperature. Thus, 380°C seemed to be suitable for PEO removal while the molten PTFE particles could have fused together and can form a continuous nanofiber structure.

In Figure 2b, the first weight losses occurred till to the 100°C of TGA curves of neat PVA and PVA/PTFE nanofibers were related to the water vaporization. The decomposition of neat PVA nanofibers began around 270°C and lost half of its mass about 355°C, leaving ~10% residue at 600°C. Neat PVA nanofibers had two degradation steps, the elimination reactions started at around 270°C till 340°C and the breakdown of the polymer backbone (mostly chain-scission reactions)^{21,32,34} started at around 400°C till maximum at 450°C as a second stage which are consistent with literature and DTG curves (Figure S2). 10PVA/PTFE, 20PVA/PTFE, 25PVA/PTFE, and 30PVA/PTFE nanofibers showed weight loss starting about 270°C (Figure S2) till 380–390°C related to the removal of PVA part and PTFE decomposition started at around 510°C. Zhou et al. investigated the sintering temperature for PVA/PTFE nanofibers and indicated 370°C as a threshold temperature, above this temperature, the PVA content did not further obviously reduce in

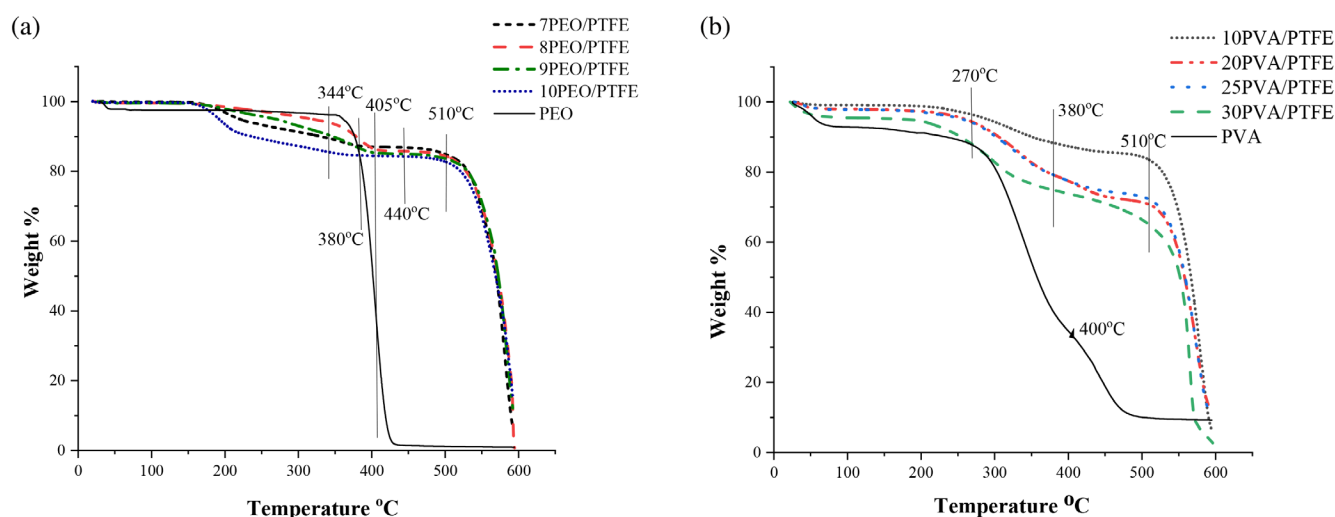


FIGURE 2 TGA curves of (a) pure PEO and PEO/PTFE nanofibers (b) pure and PVA/PTFE nanofibers. [Color figure can be viewed at wileyonlinelibrary.com]

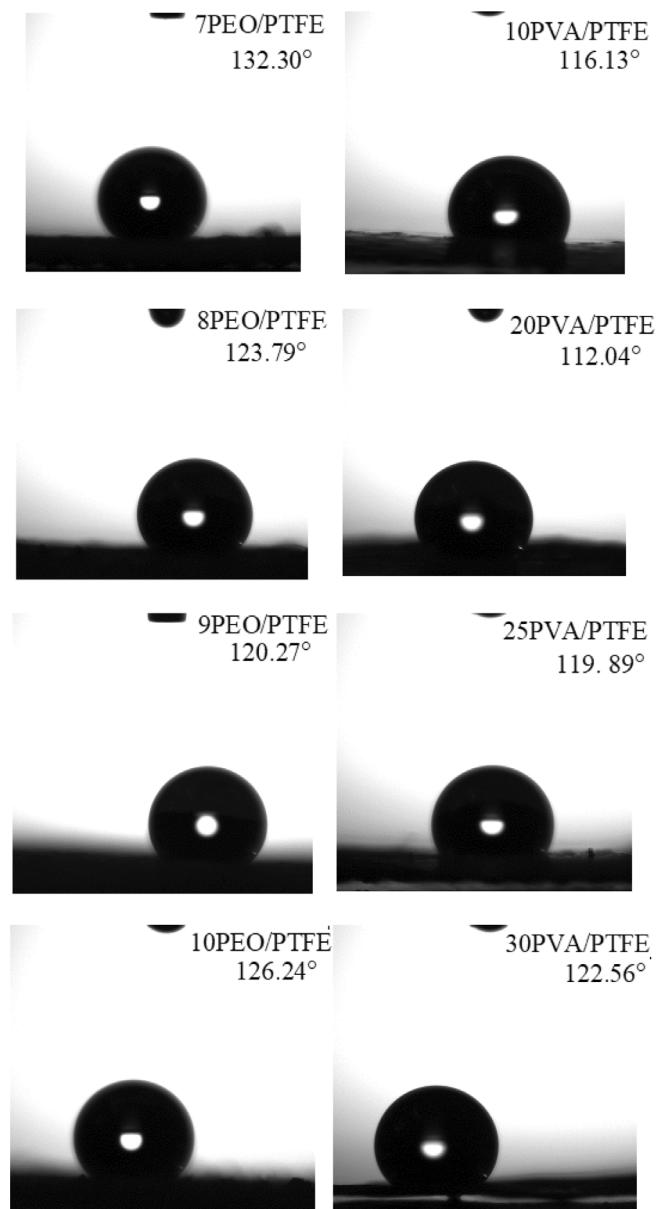


FIGURE 3 Water contact angle (°) and droplet images of PEO/PTFE and PVA/PTFE nanofibers.

the extent of 390°C.²¹ When we considered all TGA results, we decided to carry out sintering at 380°C, and by applying same sintering temperature to PEO/PTFE and PVA/PTFE nanofibers, we were able to compare the nanofiber membranes that were sintered at same temperature.

3.3 | The WCA results of nanofibers

For determination of hydrophobicity of the PTFE nanofibers, WCA values between water droplets and the PTFE nanofibers were measured and images were taken after 9 s which were also stable after this second. Water

TABLE 4 Thickness measurements of PEO/PTFE, PVA/PTFE, and commercial syringe filter membranes.

Samples	Mean thickness \pm SD (μm)
PEO/PTFE-5 h	0.24 \pm 0.031
PVA/PTFE-5 h	0.17 \pm 0.012
SF0.2	0.17 \pm 0.009
SF0.45	0.13 \pm 0.005

contact angle (°) measurement and droplet images of all concentrations were given in Figure 3. If the water contact angle is lower than 90° the surface is said to be hydrophilic and if the contact angle is higher than 90° the surface is hydrophobic according to sessile drop measurements,³⁵ so all PTFE nanofiber membranes were hydrophobic, WCA values were between 120–132° for PEO/PTFE nanofibers and 112–124° for PVA/PTFE nanofibers. Since neat PVA and PEO nanofibers were completely hydrophilic, their WCA values were 0° and not given in Table 4. PTFE amount introduced the hydrophobic effect. Since PEO part was totally removed from all PEO/PTFE nanofibers, remaining PTFE part was completely hydrophobic and small differences may be the result of surface roughness. In case of PVA/PTFE nanofibers, after sintering remaining PTFE part was again hydrophobic, all WCA measurements were higher than 90°, but when compared to PEO/PTFE nanofibers WCA measurements were slightly lower, especially for 10PVA/PTFE and 20PVA/PTFE nanofibers. As it was seen from the SEM images (Figure 5) after sintering uneven structure of the membrane might be resulted less hydrophobic PTFE membrane. According to SEM images of these nanofibers it could be seen PTFE particles bonded but smooth surface could not be achieved.

3.4 | The SEM results of nanofibers

The fiber morphology was analyzed through SEM images. The SEM images of the fiber morphologies at different weight ratios, 7/93, 8/92, 9/91, and 10/90 for PEO/PTFE and 10/90, 20/80, 25/75, and 30/70 for PVA/PTFE, before and after sintering were presented in Figure 4 and Figure 5, respectively.

In Figure 4, when the PEO ratio was the lowest (7PEO/PTFE), fibers were bead free, but PTFE particles were all on the fiber surface and some discontinuity could be seen. PTFE particles were about 140–230 nm when measured with Image J. Scale-up images can be found in supplementary file, PTFE particles along the nanofibers can be seen easily (Figure S3. and Figure S4.) At higher PEO ratios, fibers became thicker, so PTFE

particles could be dispersed more evenly along the fiber. Disregarding the PTFE particles on fiber morphology, mean nanofiber diameters were measured as 450, 524, 634, and 807 nm for 7PEO/PTFE, 8PEO/PTFE, 9PEO/PTFE, and 10PEO/PTFE, respectively. With the increasing PEO content, as expected PEO/PTFE nanofiber diameter became thicker. After sintering in all cases, connected PTFE nanofibers were achieved. Detailed images are given Again, when the PEO ratio was lowest, due to the thinner nanofiber diameter, thinner PTFE nanofibers were obtained (612 nm), when the PEO ratio was increased, more PTFE particles could be dispersed along the fiber and then they were connected after sintering which resulted in thicker and more denser PTFE nanofibers. After sintering, diameter of 7PEO/PTFE, 8PEO/PTFE, 9PEO/PTFE and 10PEO/PTFE nanofibers were 612, 818, 822, and 923 nm, respectively.

In Figure 5, PVA/PTFE nanofibers were given before and after sintering with their measured bead and nanofiber diameter. Both from the 10PVA/PTFE and 20 PVA/PTFE SEM images, it was seen that when the PVA ratio was 10 and 20%, mean nanofiber diameter were about 139 and 144, respectively and these thin nanofibers were not able to carry PTFE particles. PVA beads were measured about 497 and 549 nm, and scale-up images (Figure S4) also showed that PTFE particles could not disturbed evenly, most probably they were sprayed inside the PVA layers and after sintering they connected as a membrane without a fiber structure. When PVA ratio increased to 25%, nanofibers were able to carry PTFE particles and resulted nanofiber diameter was about 425 nm. PTFE particles were distributed along the fibers but not as even as 30PVA/PTFE nanofibers. Thus, resulted again membrane without a fiber structure after sintering. Only 30PVA/PTFE nanofibers showed some fiber structure after sintering with evenly distributed pores. Although, there were a porous structure rather than fiber, the average thickness of these fiber-like parts was 788 nm and average surface pore size was 809 nm.

When SEM images of PEO/PTFE and PVA/PTFE were compared, after sintering PEO/PTFE nanofibers preserved their fibrous structure better. Especially, 10PEO/PTFE nanofibers electrospinnability was better than other PEO/PTFE nanofibers because of higher PEO content. In case of PVA/PTFE nanofibers best spinnability belonged to 30PVA/PTFE nanofibers and preserved their fibrous structure better than other PVA/PTFE nanofibers after sintering. Thus, among PEO/PTFE and PVA/PTFE nanofibers, 10PEO/PTFE and 30PVA/PTFE nanofibers were selected for syringe filter membrane and produced for 5 h to achieve thicker membranes and coded with PEO/PTFE-5 h and PVA/PTFE-5 h.

3.5 | The FTIR and TGA results of nanofibers after sintering

The elimination of the PEO and PVA component from the nanofibers was showed with FTIR study after sintering for PEO/PTFE-5 h and PVA/PTFE-5 h membranes. FTIR spectra of these membranes were given in Figure 6a. Generally, the stretching of C—H and C—H₂ of PEO which could be found around 2888 cm⁻¹, 1466 cm⁻¹,²⁸ were absent at PEO/PTFE spectra while the most prominent peaks at 1146 and 1201 cm⁻¹ which were characteristic of CF₂ symmetric and asymmetric stretching modes could be seen. Besides, the peaks at 507, 554, and 639 cm⁻¹ could be assigned to the rocking, deformation, and wagging modes of CF₂, respectively.^{22,26,28}

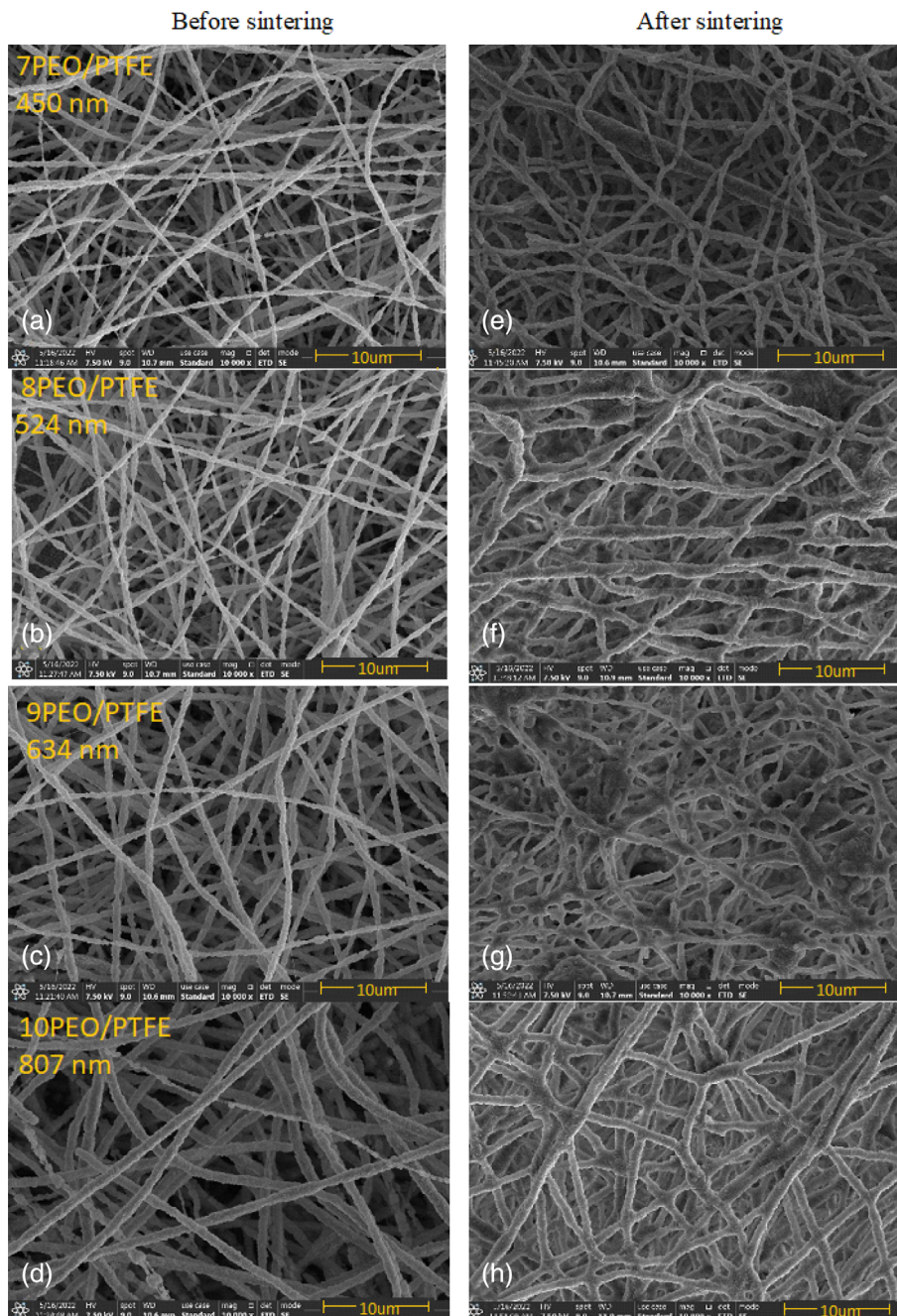
The two strong absorption bands at 1201 and 1145 cm⁻¹ which were assigned for C—F stretching vibrations were also seen in the spectra of PVA/PTFE nanofibers after sintering, while the strong absorption at 3334 cm⁻¹ which is associated with the stretching of O—H bonds for PVA was completely disappeared. However slight absorption at 2920 cm⁻¹ assigned to C—H stretching and the absorption corresponding to the CH₂ appears at about 1452 cm⁻¹^{16,21} with very low peak which was related to some residual of PVA.

This residual PVA also confirmed with TGA curves of PVA/PTFE nanofibers which was carried out after sintering again for PEO/PTFE-5 h and PVA/PTFE-5 h membranes (Figure 6b). While TGA curve of PEO/PTFE-5 h showed any degradation till 500°C which confirms total removal of PEO, TGA curve of PVA/PTFE-5 h showed approximately 8% of degradation between 420-500°C. But, as it was confirmed with WCA results, this residual did not much affect the hydrophobicity of the resultant PTFE membrane.

3.6 | The results of thickness

Thickness measurements were given in Table 4. SF0.45 membrane had a supporting thin nonwoven layer inside the syringe filter housing but measured alone. Since e-PTFE membranes are too delicate, if they need to have smaller pore size and are used without a supporting, they must be produced thicker as it is for SF0.2 membrane. When PEO/PTFE-5 h membrane compared with commercial syringe filter membranes, it was thicker (0.24 μm). PEO/PTFE-5 h membrane was also thicker than PVA/PTFE-5 h membrane because of higher PTFE content. After sintering only PTFE part remained, so it was higher for PEO/PTFE-5 h membrane. Since PTFE particles laid through the fiber structure and fused along and on the points of fiber crossovers to form an interconnected fibrous

FIGURE 4 SEM images of (a) 7PEO/PTFE, (b) 8PEO/PTFE, (c) 9PEO/PTFE, and (d) 10PEO/PTFE before and (e) 7PEO/PTFE, (f) 8PEO/PTFE, (g) 9PEO/PTFE, and (h) 10PEO/PTFE after sintering. [Color figure can be viewed at wileyonlinelibrary.com]



network, obtained membrane was thicker than expanded PTFE (ePTFE) membranes. Besides, both PEO/PTFE-5 h and PVA/PTFE-5 h membranes were easy to handle because of tougher and thicker structure.

3.7 | SEM images of commercial syringe filters and electrospun PTFE nanofibers and pore size comparison

SEM images of PEO/PTFE-5 h and PVA/PTFE-5 h membranes and two commercial syringe filter membranes, SF0.2 and SF0.45, were given in Figure 7c,d. SF0.2 and

SF0.45 membranes were ePTFE membranes and show their characteristic structure as “circumferentially arranged nodes with interconnected longitudinal fibrils”. As discussed above, PEO/PTFE-5 h preserved its fibrous structure better than PVA/PTFE-5 h and had continuous PTFE fibers with connections. Whereas PVA/PTFE-5 h had intermittent PTFE parts. Mean fiber diameters of PEO/PTFE-5 h and PVA/PTFE-5 h were measured again and was 1109 μm for PEO/PTFE-5 h and mean fiber like parts of PVA/PTFE-5 h was 968 μm , slightly higher than 1 h produced samples. Since PTFE particles fused and form fiber structure, these membranes had thicker fibers than e-PTFE membranes.

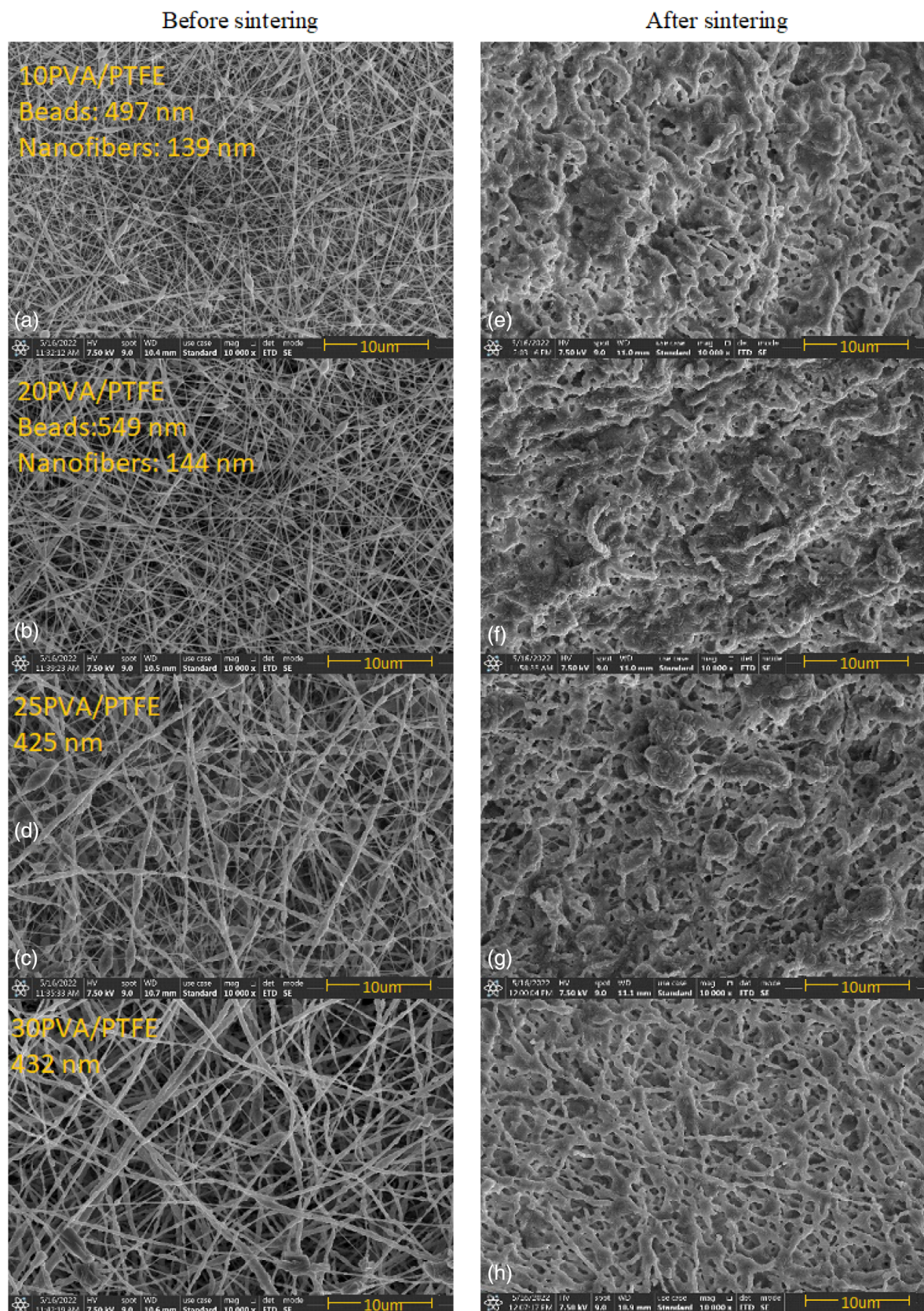


FIGURE 5 SEM images of (a) 10PVA/PTFE, (b) 20PVA/PTFE, (c) 25PVA/PTFE, and (d) 30PVA/PTFE before and (e) 10PVA/PTFE, (f) 20PVA/PTFE, (g) 25PVA/PTFE (h) 30PVA/PTFE after sintering. [Color figure can be viewed at [wileyonlinelibrary.com](https://onlinelibrary.wiley.com)]

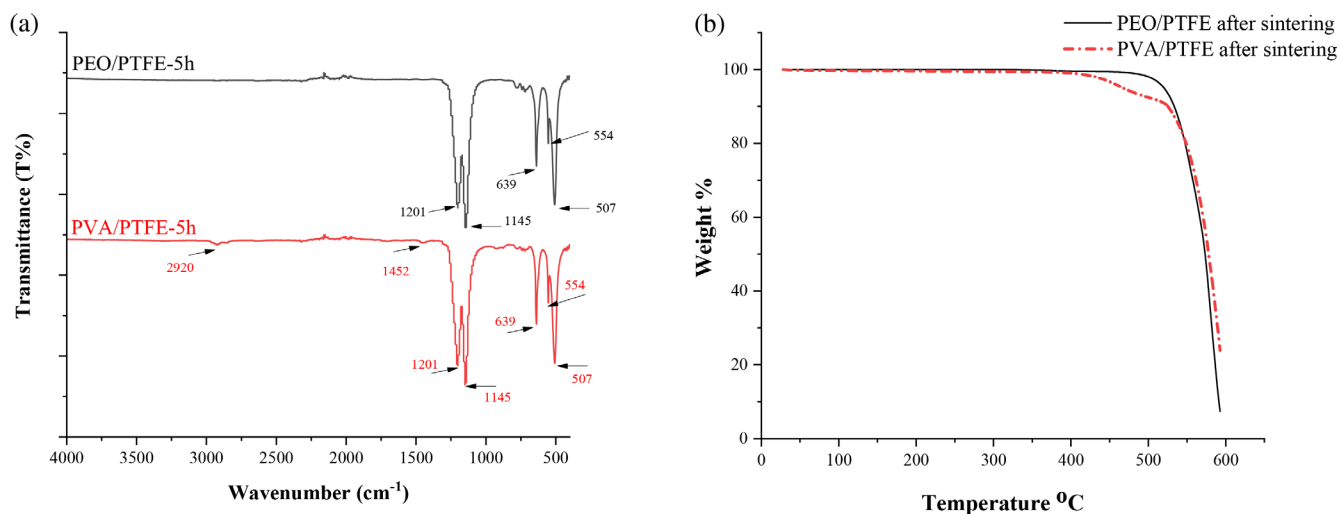


FIGURE 6 (a) FTIR spectra of PEO/PTFE and PVA/PTFE nanofibers after sintering (b) TGA curves of 5 h collected 10PEO/PTFE and 30PVA/PTFE after sintering. [Color figure can be viewed at [wileyonlinelibrary.com](https://onlinelibrary.wiley.com)]

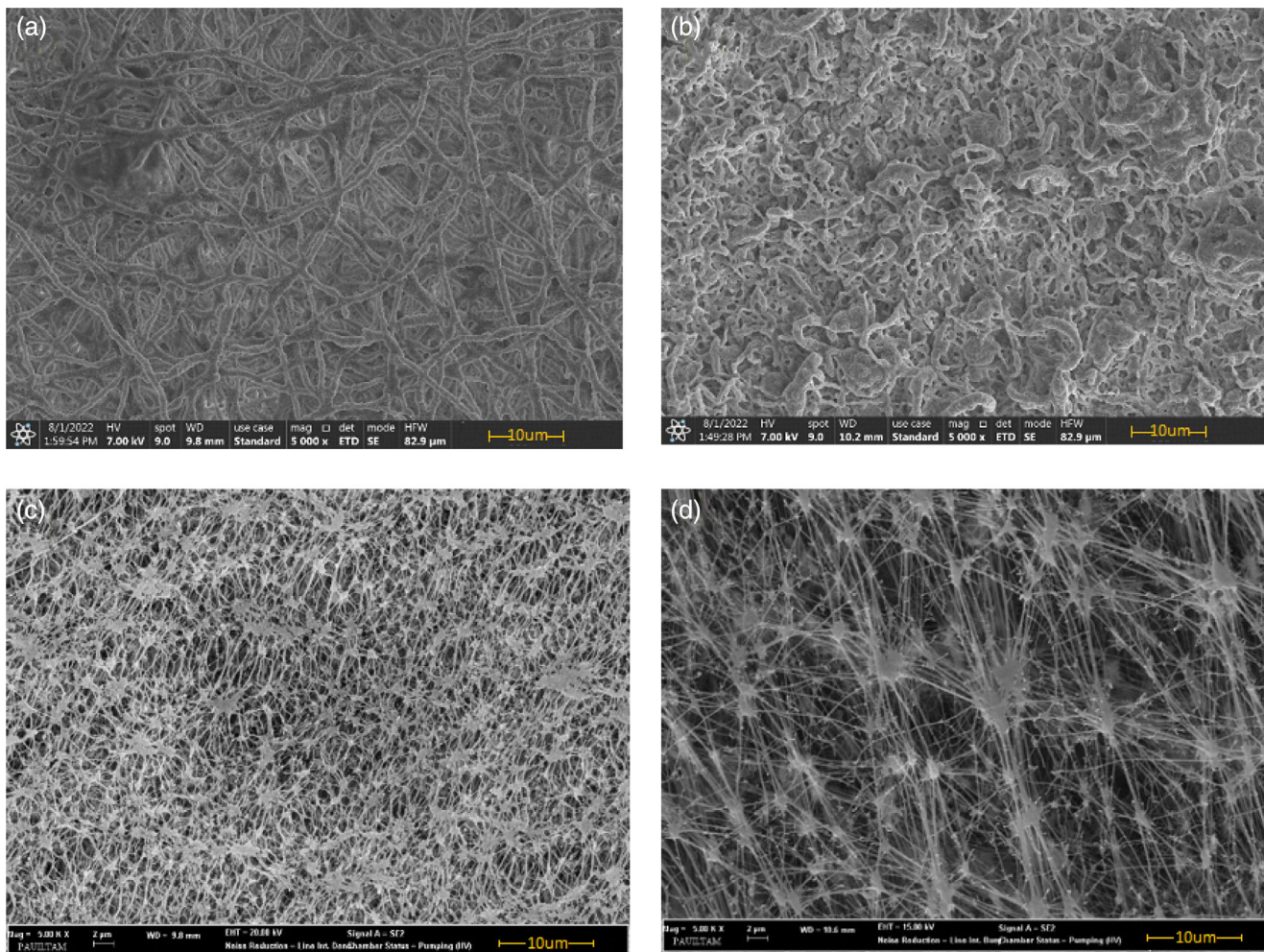


FIGURE 7 SEM images of (a) PEO/PTFE-5 h, (b) PVA/PTFE-5 h (c) SF0.2 (d) SF0.45 membrane with 5000 magnification. [Color figure can be viewed at [wileyonlinelibrary.com](https://onlinelibrary.wiley.com)]

TABLE 5 Pore size measurement, MFP, FBP, SBP of PEO/PTFE-5 h, PVA/PTFE-5 h, SF0.2 and SF0.45.

Samples	MFP (μm)	FBP (μm)	SBP (μm)
PEO/PTFE-5 h	0.90	0.90	0.85
PVA/PTFE-5 h	1.07	1.09	0.97
SF0.2	0.25	0.25	0.22
SF0.45	0.28	0.50	0.22

The vertical capillary method was performed by capillary flow porometry and pore size measurements of PEO/PTFE-5 h, PVA/PTFE-5 h, SF0.2 and SF0.45 were given in Table 5. In syringe filters, 0.2 μm membranes are typically used to remove or capture bacteria and are considered sterilizing. 0.45 μm membranes are used to remove larger bacteria or particles and are often used in water quality control testing.³⁶ Here we measured MFP of SF0.2 as 0.25 μm and SF0.45 as 0.28 μm . Since expanded PTFE membranes include nanofibrils their pore sizes are smaller and pore size distribution is narrower when compared to electrospun PTFE nanofiber membranes. Although SEM images seemed to show larger pores for SF0.45, interconnected longitudinal fibrils caused such small MFP. The pores of nanofiber membranes were caused by the entanglement of the nanofibers, with the relation of nanofiber diameter. For PEO/PTFE and PVA/PTFE membranes, the PTFE fiber diameters were approximately 1100 nm and 1000 nm, respectively; this was much higher than the nanofibrils of commercial syringe filters, hence pore size of 0.90 and 1.07 μm and higher than e-PTFE membranes.

3.8 | The results of bacterial removal

To compare the bacteria removal of PEO/PTFE and PVA/PTFE membranes with SF0.2 and SF0.45, *Escherichia coli* was prepared 8log CFU/mL and diluted to 4log CFU/mL. After filtering 10 mL of 4log CFU/mL *Escherichia coli* solutions with syringe filters, microbiological cultivation is done in a nutrient agar culture medium at 30°C and then the bacterial CFU was counted and compared with the unfiltered blank solution (Figure 8). Values are represented as log values. While blank solution that was not filtered, was counted 4.8 8log CFU/mL, PEO/PTFE-5 h was counted 1.3 3log which was very close to the 8.3 2log and 9.2 2log CFU/mL result of SF0.2 and SF0.45, respectively. However, after filtering with PVA/PTFE-5 h membrane, bacterial CFU/mL was counted 4.1 4log which was very high when compared with PEO/PTFE-5 h and commercial syringe filters. It could be assumed that the applied pressure

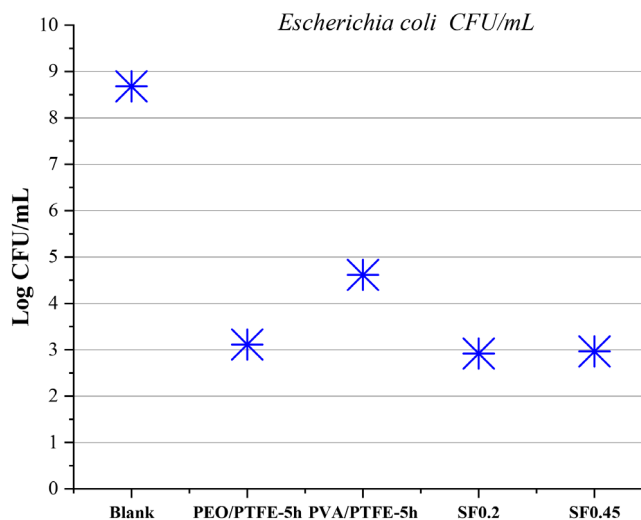


FIGURE 8 *Escherichia coli* CFU/mL after syringe filtration. [Color figure can be viewed at [wileyonlinelibrary.com](https://onlinelibrary.wiley.com/doi/10.1002/app.54544)]

causes a deformation of the PVA/PTFE-5 h membrane, maybe because of the residual PVA decrease the strength of the membrane so that the pore size increases and the bacteria leak through the membrane. Although all measured pore sizes were smaller than *Escherichia coli* size, it was not possible to filter all bacteria through the syringe filters. Possible explanation relies on the microorganisms' physiological behavior during filtration. It was reported that microorganisms are deformable under mechanical stress which leads to their internal volume reduction. It can be supposed that similar modifications occur during syringe filtration because of the applied pressure.³⁷ Nevertheless, considerable amount of bacteria could be removed with syringe filters and based on these initial bacterial removal tests with syringe filters, PEO/PTFE nanofiber membranes are promising and could be improved to be used in syringe filters.

4 | CONCLUSION

In this study, the electrospun PTFE membranes were produced by electrospinning with two carrier polymers. TGA curves of composite PEO/PTFE nanofibers showed two-step mass loss, corresponding to the decomposition of PEO and PTFE phases. The peak weight-loss temperature for the PEO component is slightly lower and about 380 °C when compared to the pure PEO and the thermal degradation of PTFE began about 510°C. After sintering, TGA curve of PEO/PTFE-5 h did not show any degradation till 510°C which confirms total removal of PEO, TGA curve of PVA/PTFE-5 h showed approximately 8% of degradation between 420-500°C due to some residual of PVA.

Nevertheless, WCA were measured between 112–132° for all PEO/PTFE, PVA/PTFE membranes. Since, there was slight residual of PVA inside the PVA/PTFE membranes and due to the uneven structure, WCA results were slightly lower than PEO/PTFE membranes. FTIR results also confirmed the total removal of PEO part, only representative peaks at 1146, 1201, 507, 554, and 639 cm⁻¹ which were belong to PTFE could be seen clearly.

Mean fiber diameters of PEO/PTFE nanofibers were between 450–807 nm and were thicker than PVA/PTFE nanofibers because of higher PTFE content and preserved their fibrous structure better. Before sintering, SEM images of PVA/PTFE nanofibers showed insufficient carrying of PTFE particles which caused uneven distribution and sticking of them after sintering. When the amount of PVA was increased to 30%, better distribution was observed through the fiber structure.

Two representative and best PTFE membranes were selected and produced at higher period, then sintered and placed inside 3D printed syringe filter housing. Produced PEO/PTFE-5 h was thicker with 0.24 μm than SF0.2 and SF0.45 commercial syringe filters. Both PEO/PTFE-5 h and PVA/PTFE-5 h membranes resulted tougher structure when compared to commercial e-PTFE membranes. MFPS were 0.90 and 1.07 μm for PEO/PTFE-5 h and PVA/PTFE-5 h, respectively and significantly higher than e-PTFE membranes. On the other hand, bacterial removal of PEO/PTFE-5 showed 1.3 3log CFU/mL *Escherichia coli*, which was very close to commercial syringe filter membranes. In case of PVA/PEO-5 h membrane it was assumed that the applied pressure caused a deformation and the bacteria leaked through the membrane. This initial bacterial removal tests showed electrospun PEO/PTFE membranes were promising and further optimization should be carried out.

AUTHOR CONTRIBUTIONS

Cigdem Akduman: Conceptualization (lead); data curation (lead); formal analysis (lead); methodology (lead); writing – original draft (lead); writing – review and editing (lead).

ACKNOWLEDGMENTS

The author would like to thank HIFYBER for pore size measurements, Sari Najdar for 3D printing of syringe filters and Ahmet Koluman (DVM, PhD) for bacterial removal tests.

FUNDING INFORMATION

The author received no financial support for the research, authorship, and/or publication of this article.

CONFLICT OF INTEREST STATEMENT

The author(s) declared no potential conflicts of interest with respect to the research, authorship, and/or publication of this article.

DATA AVAILABILITY STATEMENT

The data that support the findings of this study are available from the corresponding author upon reasonable request.

ORCID

Cigdem Akduman  <https://orcid.org/0000-0002-6379-6697>

REFERENCES

- [1] J. Smith, J. George, T. Nadler, V. Joshi, *Dissolution Technol* **2020**, *27*, 6.
- [2] Syringe Filters, <https://www.sigmaaldrich.com/TR/en/products/filtration/laboratory-syringe-filters/syringe-filters>, Accessed on 08 March 2023
- [3] Y. Huang, Q. L. Huang, H. Liu, C. X. Zhang, Y. W. You, N. N. Li, C. F. Xiao, *J. Membr. Sci.* **2017**, *523*, 317.
- [4] Syder Filtration, Definition Of Porous And Polymeric Membranes, <https://syderfiltration.com/learning-center/articles/introduction-to-membranes/polymeric-membranes-porous-non-porous/>, Accessed on 08 March 2023
- [5] S. Feng, Z. Zhong, Y. Wang, W. Xing, E. Drioli, *J. Membr. Sci.* **2018**, *549*, 332.
- [6] J. Xiong, P. Huo, F. K. Ko, *J. Mater. Res.* **2009**, *24*, 2755.
- [7] E. Shim, J. P. Jang, J. J. Moon, Y. Kim, *Polymer* **2021**, *13*, 4067.
- [8] N. Mao, J. Liu, D. Chang, X. Sun, *In 2015 International Symposium on Computers & Informatics*, Atlantis Press, Dordrecht **2015**, January, p. 2274.
- [9] D. Jiang, W. Zhang, J. Liu, W. Geng, Z. Ren, *Korean J. Chem. Eng.* **2008**, *25*, 744.
- [10] G. Liu, C. Gao, X. Li, C. Guo, Y. Chen, J. Lv, *J. Appl. Polym. Sci.* **2015**, *132*, 42696.
- [11] S. K. Biswas, K. Vijayan, *Wear* **1992**, *158*, 193.
- [12] Y. Feng, T. Xiong, S. Jiang, S. Liu, H. Hou, *RSC Adv.* **2016**, *6*, 24250.
- [13] W. Kang, H. Zhao, J. Ju, Z. Shi, C. Qiao, B. Cheng, *Fibers Polym* **2016**, *17*, 1403.
- [14] Q. Guo, Y. Huang, M. Xu, Q. Huang, J. Cheng, S. Yu, et al., *J. Membr. Sci.* **2022**, *121115*, 121115.
- [15] Uni Klinger Limited, Sintered PTFE vs ePTFE, <https://www.uniklinger.com/blog-detail/sintered-ptfe-vs-eptfe->, Accessed on 08 March 2023
- [16] Porex Filtration Group, What is the difference between ePTFE and sintered PTFE?, <https://www.porex.com/material-science/ptfe/what-is-the-difference-between-eptfe-and-sintered-ptfe/#:~:text=There%20are%20actually%20two%20types,or%20ePTFE%20%E2%80%93%20and%20sintered%20PTFE.> Accessed on 08 March 2023
- [17] Porvent, Know your PTFE: ePTFE vs. sPTFE, <https://www.porvent.com/know-your-ptfe-eptfe-vs-sptfe/>, Accessed on 08 March 2023

- [18] Inoflon Polytetrafluoroethylene Resins, Processing Guide, Free flow Granular PTFE, https://www.inoflon.com/pdf/PG_Free%20flow%20granular%20PTFE.pdf), Accessed on 08 March 2023
- [19] X. Hao, J. Zhang, Y. Guo, H. Zhang, *Int Nonwovens J* **2005**, 2, 1558.
- [20] I. Kolesnik, T. Tverdokhlebova, N. Danilenko, E. Plotnikov, D. Kulbakin, A. Zheravin, et al., *J. Fluorine Chem.* **2021**, 246, 109798.
- [21] T. Zhou, Y. Yao, R. Xiang, Y. Wu, *J. Membr. Sci.* **2014**, 453, 402.
- [22] Q. L. Huang, C. F. Xiao, X. Y. Hu, X. F. Li, *Desalination* **2011**, 277, 187.
- [23] H. Xu, W. Jin, F. Wang, G. Liu, C. Li, J. Wang, et al., *RSC Adv.* **2019**, 9, 13631.
- [24] P. Zhao, N. Soin, K. Prashanthi, J. Chen, S. Dong, E. Zhou, et al., *ACS Appl. Mater. Interfaces* **2018**, 10, 5880.
- [25] C. Su, Y. Li, H. Cao, C. Lu, Y. Li, J. Chang, F. Duan, *J. Membr. Sci.* **2019**, 583, 200.
- [26] S. Lin, Y. Cheng, X. Mo, S. Chen, Z. Xu, B. Zhou, et al., *Nano-scale Res. Lett.* **2019**, 14, 1.
- [27] A. Huang, F. Liu, Z. Cui, H. Wang, X. Song, L. Geng, et al., *Compos Sci Technol* **2021**, 214, 108980.
- [28] S. J. Son, S. K. Hong, G. Lim, *J Sens Sci Technol* **2020**, 29, 89.
- [29] Z. Q. Dong, X. H. Ma, Z. L. Xu, W. T. You, F. B. Li, *Desalination* **2014**, 347, 175.
- [30] Teflon, PTFE DISP 33, Fluoroplastic Dispersion, Product Information, <https://www.teflon.com/en/-/media/files/teflon/teflon-ptfe-disp-33-product-info.pdf?rev=5592752ad7d14b548a638988a2d64775&hash=2E32BCF24A884EAB56EEB9B4DCF51AD6#:~:text=Teflon%E2%84%A2%20PTFE%20DISP%2033%20is%20a%20milky%20white%20aqueous,adhesion%2C%20gloss%2C%20and%20weldability.>, Accessed on 08 March 2023
- [31] Dow, **2003**, POLYOX Water-Soluble Resins, Dissolving Techniques, <https://cms.chempoint.com/ic/getattachment/a9fi0764-b961-4bc9-950e-4d6e45ef53d1/attachment.aspx>, Accessed on 08 March 2023
- [32] A. Cay, M. Mirafteb, *J. Appl. Polym. Sci.* **2013**, 129, 3140.
- [33] G. J. Kim, K. O. Kim, *Sci. Rep.* **2020**, 10, 1.
- [34] T. Zhou, Q. Zhong, J. Li, Y. Yao, R. Xiang, P. Zhu, *J. Appl. Polym. Sci.* **2020**, 137, 49060.
- [35] S. S. Latthe, C. Terashima, K. Nakata, A. Fujishima, *Molecules* **2014**, 19, 4256.
- [36] ThermoFisher Scientific FAQs – FILTRATION <https://tools.thermofisher.com/content/sfs/brochures/Filtration-FAQs-June2013.pdf>, Accessed on 08 March 2023
- [37] D. Bjorge, N. Daels, S. De Vrieze, P. Dejans, T. Van Camp, W. Audenaert, et al., *Desalination* **2009**, 249, 942.

SUPPORTING INFORMATION

Additional supporting information can be found online in the Supporting Information section at the end of this article.

How to cite this article: C. Akduman, *J. Appl. Polym. Sci.* **2023**, 140(35), e54344. <https://doi.org/10.1002/app.54344>